JOURNAL OF GEOPHYSICAL RESEARCH, VOL. 108, NO. C8, 3251, doi:10.1029/2002JC001554, 2003

Near-surface circulation in the northern North Atlantic as inferred from Lagrangian drifters: Variability from the mesoscale to interannual

Philip K. Jakobsen,[1] Mads H. Ribergaard,[1,2] Detlef Quadfasel,[3] Torben Schmith,[1] and Christopher W. Hughes[4]

Received 19 July 2002; revised 24 January 2003; accepted 10 March 2003; published 5 August 2003.

[1] The near-surface circulation of the Nordic Seas is basically cyclonic and consists of jets and recirculation cells, which are tightly linked to the bottom topography. Variable forcing by the large-scale rotation of the wind leads to a modulation in the strength of the gyres and their interconnecting jets. This is seen in drifter and altimeter data. Currents are stronger during winter and during phases of high North Atlantic Oscillation Index. The exchanges between the North Atlantic and the Nordic Seas do not seem to be directly affected by this variable forcing. The narrow boundary currents and the intergyre jets are subject to instability, causing mesoscale current fluctuations, which contribute to the stirring and mixing of Polar and Atlantic water masses. *INDEX TERMS:* 4243 Oceanography: General: Marginal and semienclosed seas; 4520 Oceanography: Physical: Eddies and mesoscale processes; 4532 Oceanography: Physical: General circulation; 4215 Oceanography: General: Climate and interannual variability (3309); *KEYWORDS:* mesoscale eddies, North Atlantic, Nordic Seas, surface circulation, surface drifters, variability

Citation: Jakobsen, P. K., M. H. Ribergaard, D. Quadfasel, T. Schmith, and C. W. Hughes, Near-surface circulation in the northern North Atlantic as inferred from Lagrangian drifters: Variability from the mesoscale to interannual, *J. Geophys. Res.*, *108*(C8), 3251, doi:10.1029/2002JC001554, 2003.

1. Introduction

[2] The Arctic Mediterranean is a kitchen for deepwater formation and therefore plays a role in our climate system. Through shelf-slope and through open ocean convection it provides the source for the dense overflow waters that enter the North Atlantic across the Greenland-Scotland Ridge. These overflows are the nucleus of the North Atlantic deep water, which is a main water mass of the global deep circulation. The surface circulation of the Nordic Seas is largely meridional. Warm and saline Atlantic water flows northward in the Norwegian Atlantic Current in the east of the Nordic Seas; the East Greenland Current in the west carries cold and low-salinity polar water, and exports a large fraction of the freshwater that has entered the Arctic Mediterranean from the atmosphere and via rivers. In between the two boundary currents a series of cyclonic gyres exist that is linked to the local bottom topography [*Poulain et al.*, 1996a]. The role of the circulation is threefold: (1) through doming of the stratification it determines the sites of convection, (2) it supplies the source waters, and (3) exports the transformed waters in the boundary currents. About three quarters of the inflowing Atlantic water leave the region in the deep overflows and about one quarter near the surface in the East Greenland Current [*Hansen and Østerhus*, 2000].

[3] South of the ridge system the topographic steering of the flow is still observed, albeit somewhat less pronounced in the east [*Otto and van Aken*, 1996]. The Atlantic inflow follows several pathways, along the European continental slope and the mid-Atlantic Ridge, but has a broader and sluggish character in between these two branches over the Icelandic Basin [*McCartney and Mauritzen*, 2001]. Most of the Irminger Current branch in the west recirculates cyclonically south of Iceland, joins the East Greenland Current, and rounds the Labrador Sea [*Cuny et al.*, 2001], which hosts the second major deepwater formation region of the North Atlantic [*Marshall and Schott*, 1999]. Here upper North Atlantic deep water is formed.

[4] Much of the present-day knowledge about the circulation in the Nordic Seas and North Atlantic is based on water mass analysis, with important contributions going back more than a hundred years [*Petterson*, 1900; *Helland-Hansen and Nansen*, 1909]. Today hydrographic data still provide a basis for circulation studies [*Björk et al.*, 2001; *Rhein et al.*, 2002], although during the last decades or so more and more direct current observations have become available. Moored instrumentation, but mainly surface drifters and deep floats have contributed to a more detailed description of the circulation [*Krauss*, 1995; *Poulain et al.*,

[1]Danish Meteorological Institute, Copenhagen, Denmark.
[2]Formerly at Greenland Institute for Natural Resources, Nuuk, Greenland.
[3]Niels Bohr Institute for Astronomy, Physics and Geophysics, Department of Geophysics, University of Copenhagen, Copenhagen, Denmark.
[4]Proudman Oceanographic Laboratory, Prenton, UK.

0148-0227/03/2002JC001554$09.00

1996a; *Fratantoni*, 2001; *Lavender et al.*, 2000; *Cuny et al.*, 2001]. These studies show many details in the circulation, with a main finding that the barotropic component of the flow and the associated topographic steering dominate the mean circulation.

[5] When it comes to the variability of the large-scale circulation, the information provided in the literature is much less conclusive. *Poulain et al.* [1996a] state that "their present data set is not well suited to the study of overall seasonal variability in the Nordic Seas" and also *Fratantoni* [2001] refrained from analyzing variability beyond that associated with synoptic scale eddies in his 10-year data set. Also, studies of the interannual variability of the flow that might be related to climate variability or decadal scale oscillations had so far to rely on hydrographic data and moored observations, because drifter and float data sets were sparse.

[6] Additional drifter data have accumulated since the studies mentioned above were done and here we investigate the variability of the circulation on timescales between weeks and several years. The Lagrangian current measurements were made during the period 1990–2000. Our main area of interest is the Nordic Seas, but we cover the whole Atlantic north of 50°N, which enables us to discuss the circulation in a larger context.

[7] The following aspects or questions motivated our study:

[8] (1) Several model studies on the circulation covering this region have been and are being carried out. With our analysis we want to provide a reference against which simulation results can be tested. The current fields will also be used to study the drift of fish larvae from the spawning to the nursery grounds to shed insight into observed variability in fishery productivity.

[9] (2) The wind forcing over the Nordic Seas undergoes strong seasonal and also interannual variability, but the exchanges between the Nordic Seas and the North Atlantic appear to be remarkably stable. Is the response of the circulation confined to the internal gyre recirculations?

[10] (3) The generation of fronts and the stirring through mesoscale eddies lead to enhanced mixing of water masses. What is the implication of this mixing on the large-scale circulation?

[11] The paper is organized as follows. Section 2 gives an overview of the data material and the basic analysis methods. Sections 3–5 present the mean structure of the circulation, its variability on seasonal and interannual timescales, and its mesoscale variability. In section 6 we discuss implications of the results with respect to the questions posed above.

2. Data and Methods

2.1. Drifter Data

[12] The drifter data set comprises more than 81,000 buoy days of position collected with 387 WOCE/TOGA type drifters drogued at 15 m depth during the 1990s. The slippage on the drifters due to transfer of momentum to the surface buoy from waves and wind is minimized through their design and estimated to be less than 1 cm/s in winds of 10 m/s [*Niiler et al.*, 1996]. This error is about as large as that associated with the satellite positioning. Initial processing of the data included quality control and interpolation of the positions at 6-hour intervals and is described in detail by *Hansen and Poulain* [1996] and *Poulain et al.* [1996b]. This basic data set is available from the Drifting Buoy Data Assembly Centre at http://www.aoml.noaa.gov. For our analysis we only used those parts of the position time series when the drogue was attached to the drifter [*Poulain et al.*, 1996b; *Jakobsen*, 2000]. The time series of positions were low-pass filtered to eliminate semidiurnal tidal and inertial period waves, and entered the analysis when the remaining length was longer than 30 days. This latter condition is required by the additional filtering procedures described below.

[13] With their drogues located at 15 m depth the drifters are carried not only by the geostrophic flow, but also by Ekman currents. The wind stress field over the Nordic Seas is dominated by synoptic scale variability with typical timescales of a few days. Consequently, steady Ekman currents will not be set up, but instead the mixed layer will be dominated by inertial oscillations. These are filtered out along with the tidal movements, but the mean wind above the synoptic scale gives rise to a residual mean Ekman current. The drifter movement to such a current is found to scale with 0.5% of the wind speed for the WOCE/TOGA type drifter [*Niiler and Paduan*, 1995; *Poulain et al.*, 1996a]. In the Nordic Seas the climatological wind is on the order of 4 m/s [*Kistler et al.*, 2001] which gives rise to a mean Ekman current on the order of 2 cm/s largely perpendicular to the isobaths (Figure 1). We expect to monitor mainly the geostrophic flow as the drifters generally follow the isobaths (Figure 6).

[14] The distribution of data is not homogeneous either in time or in space (Figure 2). The SACLANT buoy programme [*Poulain et al.*, 1996b] during the first half of the 1990s focused on the Nordic Seas, while WOCE efforts concentrated in the North Atlantic during the second half of the decade. Also, the Lagrangian nature of the measurements contributed to the inhomogeneous data distribution. In particular, there are very little data in the East Greenland Current, due to the presence of ice in this area.

[15] To get pseudo-Eulerian maps (see below) we average over 1° latitude × 2° longitude boxes, a scale well above the internal radius of deformation, and shift our averaging boxes by half the box size in each direction. This gives a resolution of about 50 km, but since the boxes overlap, the field is somewhat smoothed.

2.1.1. Separation of Scales: Mesoscale Variability

[16] A by-product of the calculation of the Eulerian mean velocity is an estimate of the fluctuation velocity usually taken as the difference between the box mean and the individual velocity data. This fluctuation velocity is commonly expressed in terms of a standard deviation or of a fluctuation kinetic energy. It does contain the whole spectrum of deviations from the mean, from high-frequency waves to interannual fluctuations. Since the mean is taken over a limited size spatial box, these fluctuations are often associated with the high-frequency part of the spectrum, i.e., the mesoscale or synoptic scale variability, but strictly speaking this is not true.

[17] To avoid this problem, we separate the different processes in the time domain rather than in space. This can easily be done with the individual drifter records by

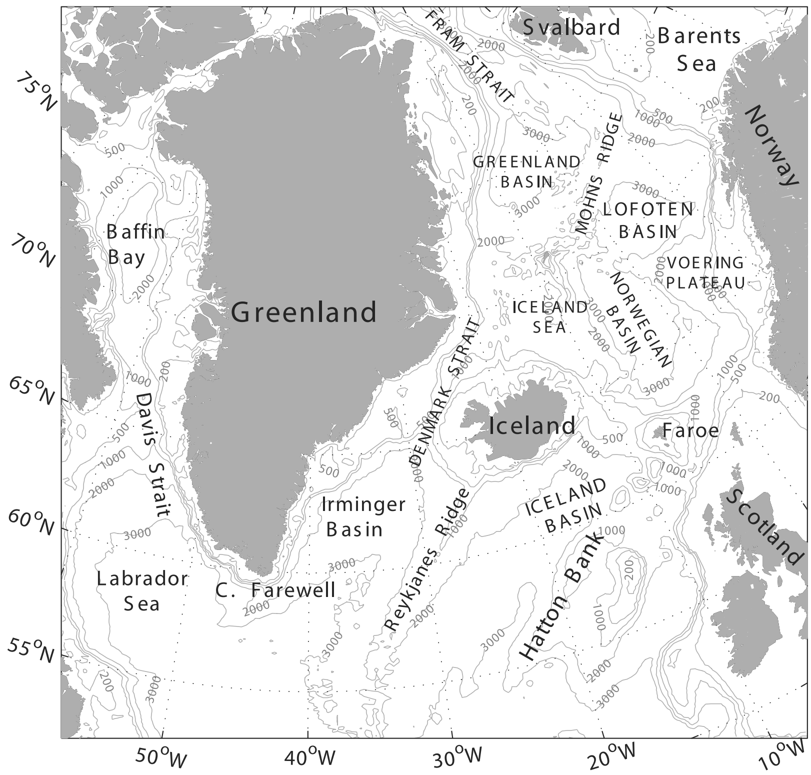

Figure 1. Bathymetry of the area of investigation. The 200, 500, 1000, 2000, and 3000 m isobaths are shown.

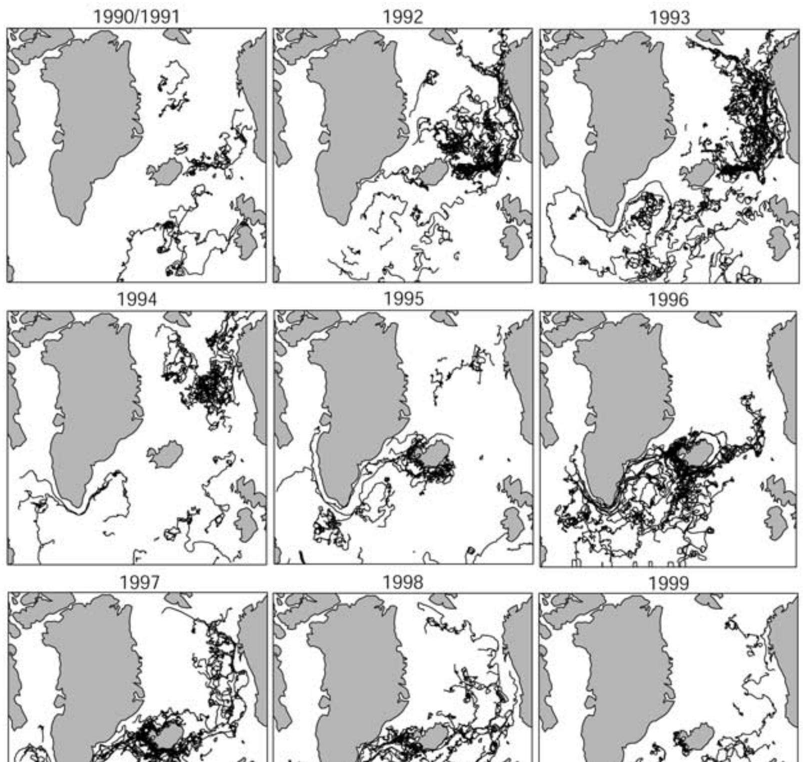

Figure 2. Trajectories of all drifters during the years indicated. During the first half of the decade, data availability is higher in the Nordic Seas; during the second half it is higher in the North Atlantic.

applying a filter in time to either the positions or the velocities. However, we first have to determine the separation scale between mean and mesoscale velocities. Following the theory of geostrophic turbulence, mesoscale eddies scale with the deformation radius L_D [*Kamenkovich et al.*, 1986; *Pedlosky*, 1987]. *Cushman-Roisin and Tang* [1990] supported this through a series of numerical experiments and found a statistical equilibrium at 2–4 L_D. Studies using TOPEX/Poseidon altimeter derived sea surface heights also showed the inferred length scale to be around 2 L_D [*Stammer*, 1998]. Using the deformation radii compiled by *Chelton et al.* [1998] implies that in the Nordic Seas mesoscale eddies can be expected to exist at spatial scales between 10 and 60 km. Direct observations support this range estimate [*Marshall and Schott*, 1999; *Van Aken et al.*, 1991]. *Poulain et al.* [1996a] found Eulerian length scales of 20–30 km using drifters. It is thus very unlikely that one single time separation for mesoscale fluctuations exists, and indeed the energy spectra and the distribution of high-frequency kinetic energy as a function of the filter cutoff period do not show such a clear separation time. Since the expected fluctuation velocities associated with the mesoscale eddies are on the order of 5–10 cm/s, corresponding to a time of rotation of 10–20 days, we somewhat arbitrarily chose a filter cutoff period of 18 days to separate the mesoscale eddies from the mean and the low-frequency fluctuating current field. We repeated our calculation with a period of 40 days which elevated the level of fluctuation energy, but did not change its relative distribution.

[18] For our analysis the individual drifter time series was thus filtered with a cutoff period of 18 days, the high-frequency part being associated with mesoscale variability, and the low-frequency part with the mean and seasonal and interannual changes.

2.1.2. Eulerian Averages: The Mean Flow

[19] The transformation of Lagrangian data into Eulerian averages is far from trivial [*Davis*, 1994; *Garraffo et al.*, 2001b]. The drifters tend to diffuse down the gradient of the data concentration and thereby induce a spurious flow perpendicular to the mean flow. Following *Davis* [1994] this bias is estimated as $U_B = -\mathsf{K}(\nabla C/C)$ where C is the data concentration and K is the drifter diffusivity tensor. We disregard the off-diagonals and estimate $K_{uu} = \langle u'u' \rangle T_u$ and $K_{vv} = \langle v'v' \rangle T_v$ [*Lumpkin et al.*, 2002] where $\mathbf{T} = (T_u, T_v)$ is the Lagrangian velocity timescale defined as:

$$T_u = \frac{1}{\sigma_u^2} \int_0^\infty R_{uu}(\tau) d\tau, \; T_v = \frac{1}{\sigma_v^2} \int_0^\infty R_{vv}(\tau) d\tau.$$

Here σ^2 is the variance and R is the Lagrangian temporal autocovariance function. The timescales are estimated using the procedure given by *Garraffo et al.* [2001a]. In general we find that the bias velocities are insignificant, except at the rim of our data set, where they can be up to a few cm/s, like in the East Greenland Current. We corrected our mean velocity estimates with respect to the bias.

[20] There are two ways of calculating the Eulerian bin average: One can treat all individual 6-hourly data with equal weight; or one can average data from the individual drifter segments and then estimate the bin average as the mean of these. For our data set the two methods give similar results for the direction of the mean current, but the first method results in about 20% lower speeds, as it over-represents slow-moving drifters in the statistics. Throughout this paper we first treat the individual drifter segments individually before calculating ensemble statistics.

[21] The standard error of the so averaged velocities is estimated as $Er = (\sigma/\sqrt{N^*})$, where $N^* \approx N\Delta t/2T$ is the number of independent measurements [*Garraffo et al.*, 2001b], with Δt as the sampling interval and T as the Lagrangian timescale. Standard errors are small compared to the mean flow except in regions with poor data coverage (Figure 3). The relatively low overall error margins are of course a consequence of the prior removal of mesoscale variability.

[22] We also considered another binning technique applied by *Davis* [1998] to subsurface float data in the South Pacific and more recently by *Fischer and Schott* [2002] to float data in the Labrador Sea. The method assumes a dominance of the barotropic flow and thus a preferential drift along lines of constant f/H, where H is the water depth and f is the Coriolis parameter. Such an assumption is certainly valid in the North Atlantic where stratification is weak. Averaging here is not done in square boxes, but in elongated areas stretching along lines of constant water depth. We applied the method to the near-surface drifters, but it turned out that the results did not significantly differ from those of the "moving current meter" method, even though a wide range of shapes was tried. This is likely due to the relatively high data concentration and our choice of relatively small averaging boxes that resolve the major topographic features.

2.2. Wind Stress Data

[23] The wind stress curl is calculated from 6-hourly wind stress data provided in the NCEP/NCAR reanalysis project at http://www.cdc.noaa.gov [*Kistler et al.*, 2001]. The reanalyses are produced by passing all available historical atmospheric observations from the reanalysis period through a data assimilation and analysis system analogous with the systems used for weather prediction. In this way one obtains a more homogeneous analysis of the atmospheric state than using products from weather prediction systems, where the data assimilation and analysis procedure have undergone changes through time. On the other hand, this does not mean that the reanalysis is without inhomogeneities, but these are due to changes in observation coverage, the most dramatic being due to the introduction of space-borne instrumentation.

[24] The different products from the reanalysis do have different levels of reliability. Observed values of mean sea level pressure, geopotential heights, and free atmospheric temperatures are directly assimilated into the model, and the reanalysis of these fields are therefore strongly influenced by observations. Surface fluxes like the wind stress are, in contrast, diagnostically calculated from the free atmospheric fields and the surface conditions such as temperature and sea ice coverage.

2.3. Altimeter Data

[25] The annual cycle of sea surface height, after correction for the inverse barometer effect to make it representative of geostrophic currents, was calculated by least squares fitting of sine and cosine functions, to the 0.25° gridded

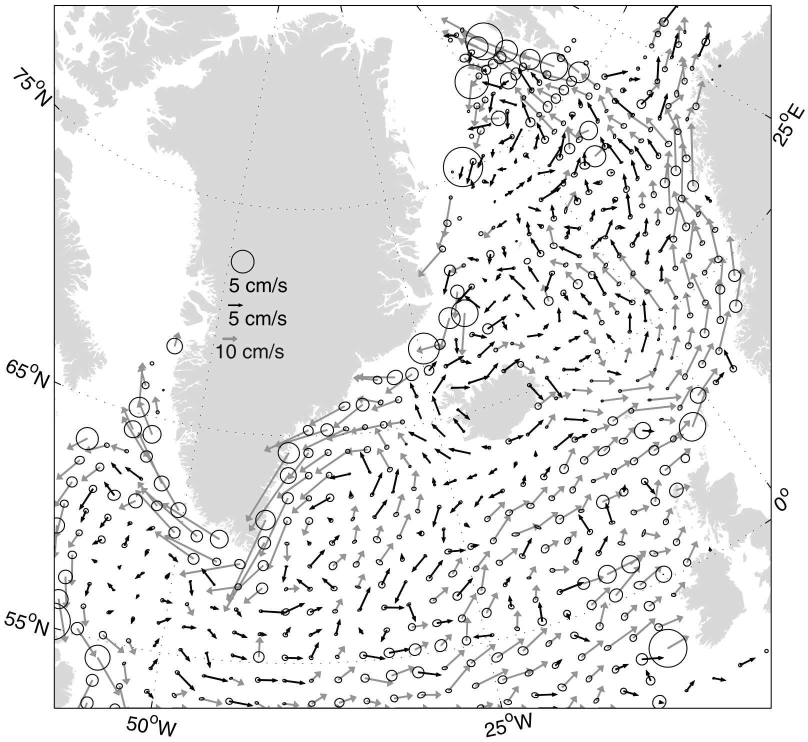

Figure 3. Quasi-Eulerian current vectors derived from 18 day low-passed filtered trajectories with standard error ellipses. See text for details of the data treatment.

maps of *Le Traon et al.* [1998]. These maps combine ERS and TOPEX/Poseidon (T/P) altimetry into a map every 10 days from 22 October 1992 to 6 August 2001. However, only *T*/*P* altimetry was available from January 1994 to March 1995, limiting latitudinal coverage during this period to the region south of 66°N. The maps were produced by an objective mapping method, which takes account of the correlation of errors in the long track direction. In the region considered here it assumes a simple isotropic form for the spatial correlation of sea surface height with a zero-crossing distance decreasing of 100 km. The correlation function in time is Gaussian with an e-folding scale of 15 days.

[26] With a typical between-track spacing of 40 km, and time between measurements varying from 5 to 35 days (depending on position) the maps are expected to capture most of the variability in this region, although some mesoscale will be missed. According to *Ducet et al.* [2000], mapping errors in this region are less than or about 20% of signal variance, except in the shelf region where high-frequency storm surges dominate. The annual cycle should be better determined as it is not dominated by the mesoscale and is resolved in time.

[27] Standard errors in the fitted annual cycle, based on a 4-cm white noise error in the individual maps, are 0.32 cm for each component (sine and cosine). Errors are therefore dominated by leakage of near-annual, nonperiodic signals into the annual cycle, an error source difficult to assess for either altimetry or drifters.

3. Mean Circulation

3.1. Major Current Systems

[28] Drifter data from the North Atlantic obtained during the past two decades have been described by several authors putting emphasis on different aspects of the circulation. *Poulain et al.* [1996a] described the circulation north of the Greenland-Scotland Ridge and identified four recirculation gyres in between the two meridional boundary currents. *Fratantoni* [2001] deals with the circulation south of the ridge and identifies the three main inflow branches of

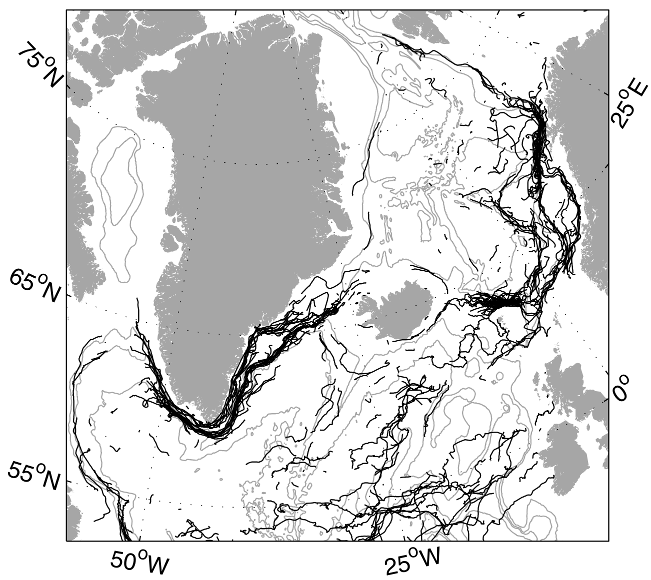

Figure 4. Trajectories of fast moving drifters during 1990–2000. To remove the mesoscale noise from the picture, trajectories are only shown if the 40 day low-pass filtered velocity is larger than 18 cm/s. Strongest flow is observed in the two meridional boundary currents and their branches.

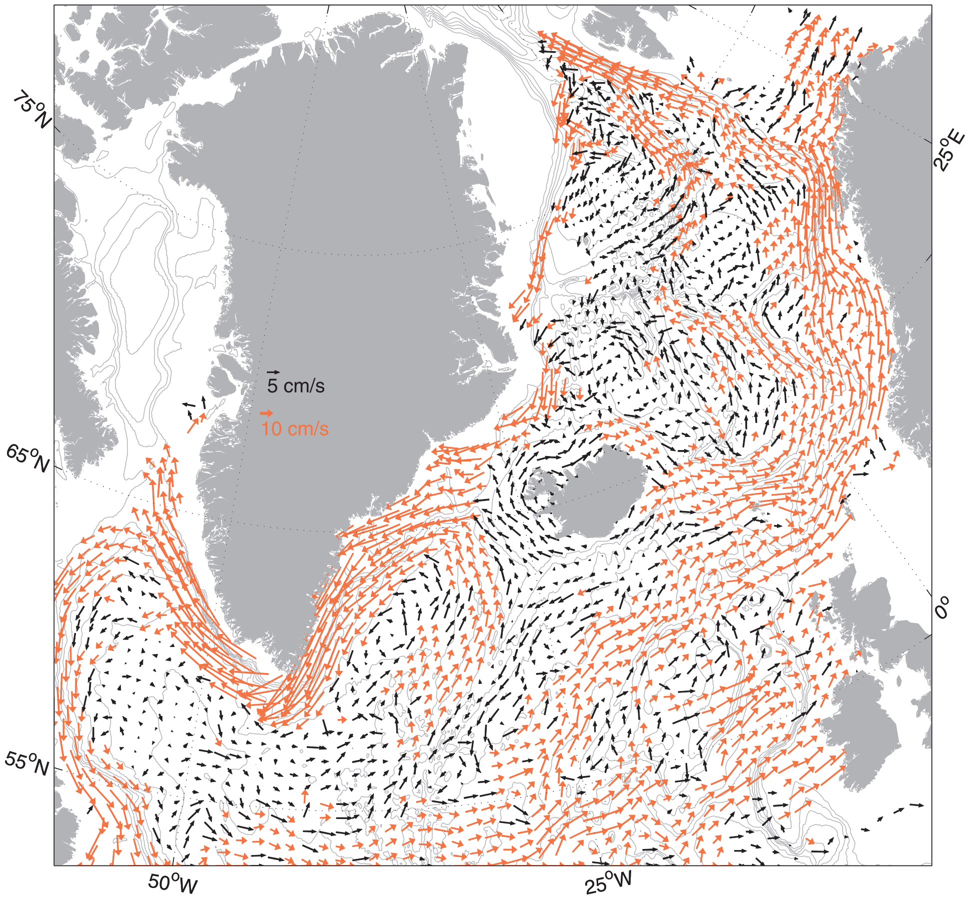

Figure 5. Quasi-Eulerian current vectors derived from 18 day low-passed filtered trajectories and averaged in overlapping 1° latitude × 2° longitude boxes. See text for details of the data treatment. Note the different scales for low-velocity (black arrows) and high-velocity currents (red arrows). Bottom topography at 500 m intervals is shown as gray lines.

Atlantic water into the Nordic Seas, while *Orvik and Niiler* [2002] explore the paths of Atlantic waters north of the ridge. These papers confirm earlier studies based mainly on hydrographic data [*Hansen and Østerhus*, 2000; *McCartney and Mauritzen*, 2002]. We will therefore describe the mean circulation only briefly.

[29] The major features of the large-scale circulation can be identified by looking at a selection of drifter trajectories (Figure 4) and at the pseudo-Eulerian vector map (Figure 5). The North Atlantic Current crosses the mid-Atlantic Ridge near 53°N and splits into the three major branches, feeding the Irminger Current in the west, the Faroe Current via the exchange across the Iceland-Faroe Ridge, and the Slope Current along the European continental slope. North of the ridge the Norwegian Atlantic Current also has different branches, as discussed by *Poulain et al.* [1996a], *Orvik et al.* [2001], and *Mork and Blindheim* [2000]. Here the westernmost one is a continuation of the Faroe Current and is steered by the Vøring Plateau, following approximately the 2000-m isobath. Some of the water follows this isobath around the southern rim of the Lofoten Basin toward Norway, but most of it continues northwest toward the Greenland Basin contributing to the Arctic Front along the Mohn Ridge [*Orvik and Niiler*, 2002]. Most of the inflow in the slope current between Faroe and Shetland continues north following the continental slope of Norway. The West Spitsbergen Current off the Barentsshelf and Svalbard is a continuation of this branch. Off the Norwegian coast there is a third current system. This is not a part of the Norwegian Atlantic Current system but rather the baroclinic Norwegian Coastal Current, driven by freshwater discharge from the Baltic and the Norwegian fjords [*Orvik et al.*, 2001]. However, the drifter tracks suggest that some interchange between these Norwegian current branches occurs. This will be shown later when discussing eddy fluxes.

[30] The East Greenland Current north of Denmark Strait can hardly be identified in our data, due to poor data coverage in the area, which is caused by the heavy concentration of multiyear ice advected southward from the Arctic Ocean. In Denmark Strait the flow has a strong westward component showing the influence of the recirculation of the Irminger Current rather than the East Greenland Current. Just south of Denmark Strait there exist two branches of surface flows side by side, which may be associated with the East Greenland Current and the above mentioned recirculation, respectively. High-resolution hydrographic and current measurements on the shelf and slope confirm this picture [*Pickart*, 2000]. As the two branches flow around Cape Farewell they combine when the Irminger Current subducts under the low-salinity Polar water of the West Greenland Current. Most of the drifters follow the bottom topography and recirculate in the Labra-

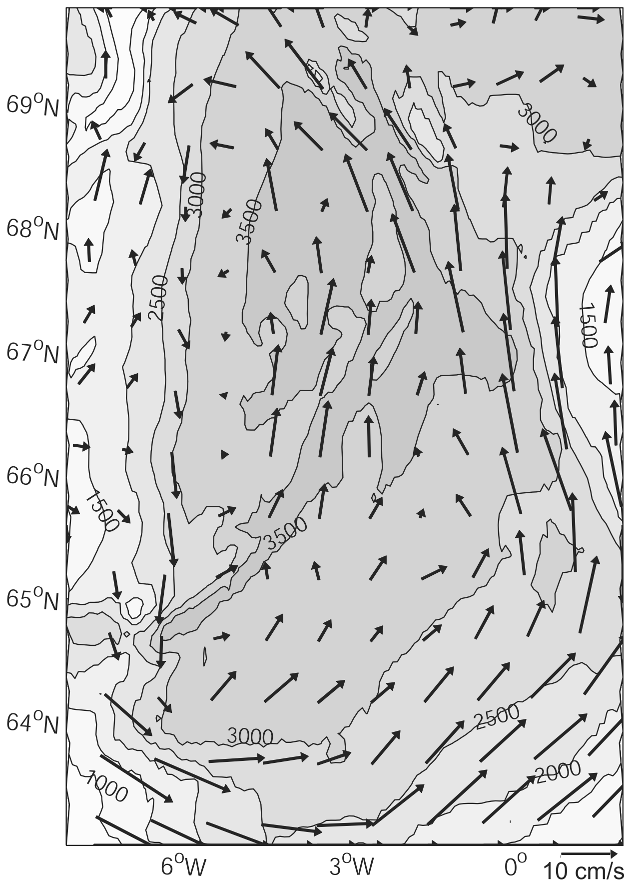

Figure 6. Detailed map of bottom topography and quasi-Eulerian current vectors from a region in the central Nordic Seas (Norwegian Basin), illustrating the barotropic nature of the circulation. Bottom topography is contoured at 500 m intervals.

dor Sea [*Fratantoni*, 2001], but a few also make it through Davis Strait into Baffin Bay. In a hydrographic section off Cape Farewell *Bacon et al.* [2002] find the subducted Irminger Current at around 75 m depth and a freshwater jet further inshore, which they name the East Greenland Coastal Current. In this new nomenclature our inner branch (Figure 4) would be the coastal current.

3.2. Flow Across the Greenland-Scotland Ridge

[31] A remarkable feature of the exchanges across the Greenland-Scotland Ridge is their steadiness on timescales above mesoscale (>12 days) [*Hansen and Østerhus*, 2000; *Dickson and Brown*, 1994]. The deep fluxes in the overflows are limited by hydraulic control, which, for reasons of continuity in turn also limits the upper layer exchanges. This implies that the circulation over the ridges is characterized by strong recirculations guided by the local topography. This is particularly evident in Denmark Strait (Figure 5). The Irminger Current flows northward along the flank of the mid-Atlantic Ridge and deflects westward when approaching the strait. Of course, some of the warm Atlantic water continues northward along the Icelandic shelf and slope, but its net transport into the Nordic Seas is only about 1 Sv (1 Sv = 10^6 m^3/s) compared to more than 8 Sv further south [*Krauss*, 1995; *Hansen and Østerhus*, 2000]. Indeed, in our data set all drifters observed in the East Greenland Current south of Denmark Strait originate from the Irminger Current. Most drifters recirculate within Denmark Strait, some north of it, but only very few south of the strait. Another important aspect of the strong cyclonic gyre in the Irminger Sea is the associated doming of its stratification. *Pickart* [2000] suspected this doming combined with strong heat fluxes to lead to deep convection during winter, similar but separated from that in the Labrador Sea.

[32] The situation is different over the eastern part of the ridge system (Figure 5). The central Atlantic water branch follows the eastern part of the Iceland Basin, northwest of Hatton Bank, and along the chain of northern banks toward the Faroe Islands. The recirculation here is less pronounced, there is some return flow along the eastern flank of the Reykjanes Ridge, but most water continues and crosses the Island-Faroe Ridge to feed the Faroe Current. Earlier studies using shipboard current profile measurements indicated a clockwise circulation on the ridge, with most of the fluxes across occurring close to Iceland [*Hansen and Meincke*, 1979], but our data indicate a broad, almost zonal flow across the entire length of the ridge. This indicates that at the sea surface the baroclinic flow associated with the Polar Front dominates over the topographic steering of the barotropic currents. The Wyville-Thomson Ridge at 60°N, 8°W lies perpendicular to the continental slope and also acts as a guide for the Atlantic inflow into the Nordic Seas. It funnels the broad zonal flow further offshore which then feeds into the narrow slope current. No recirculation toward the south can be seen in this eastern part of the ridge.

3.3. The Nordic Sea Gyres

[33] With more and more data becoming available a more detailed picture of the circulation emerged. Early work by *Petterson* [1900] based on a few hydrographic sections showed just one large-scale cyclonic gyre, whereas a century later *Poulain et al.* [1996a] already saw four different topographically steered swirls to populate the Nordic Seas. These are the gyres in the Greenland, Lofoten, and Norwegian Basins, and that of the Islandic Plateau. The almost perfect match of the flow field with the bottom topography is illustrated in Figure 6 for the central Nordic Seas: each of the gyres has a cyclonic circulation with the boundary or topographically steered currents touching and connecting the gyres. We believe that these intergyre jets are responsible for the larger-scale transport of heat and freshwater, whereas the gyres themselves mainly contribute to the mixing and transformation of water masses. Since the bottom topography of the North Atlantic is known down to scales of a few kilometres, it seems unlikely that more and new gyres will be discovered in the future. The focus of our work thus concerns the variability of the flow field and the relation of the intergyre jets with the gyre circulation itself.

[34] An example for such variability was reported by *Orvik et al.* [2001] who found seasonal transport changes between 3 Sv in summer and 8 Sv in winter in the Norwegian Atlantic Current about 400 km downstream of the Faroe Islands. Likewise, *Woodgate et al.* [1999] found seasonal changes between 11 and 37 Sv in the transport in the East Greenland Current near 75°N in the Greenland Sea. As such large variability has never been observed in the import and export rates of water from and to the North

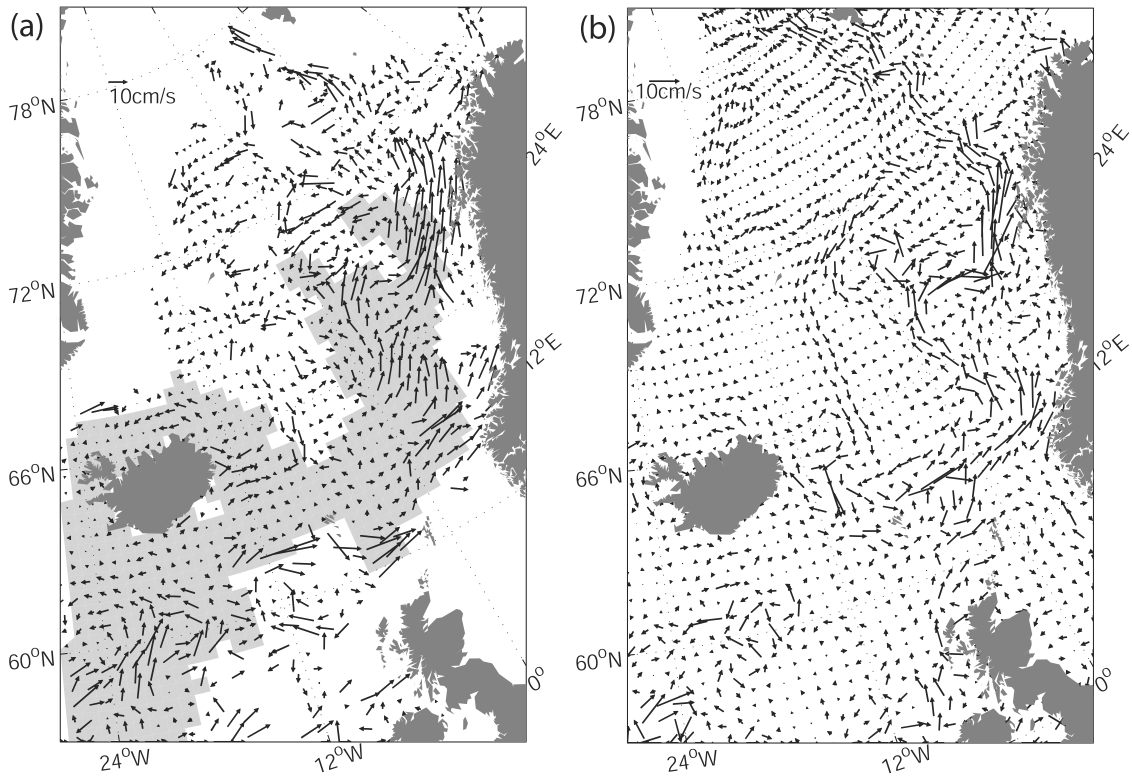

Figure 7. (a) Seasonal variation of the quasi-Eulerian near-surface currents calculated as the difference between winter (November–April) and summer (May–October). Only those regions are shown where at least 50 data points are available during both seasons and during both periods 1991–1995 and 1996–1999. The shading indicates areas where the difference is statistically significant to the 5% level based on the vectorial *t*-test described by *Garraffo et al.* [2001a]. (b) Winter minus summer mean geostrophic velocity estimated from ERS and TOPEX/Poseidon altimetry from 1992 to 2002. Please note the different scaling compared to Figure 7a.

Atlantic, it can therefore only be due to a varying internal gyre circulation.

4. Seasonal and Interannual Variability

[35] We estimate the spatial distribution of this seasonal variability from the drifter data by subtracting the mean Eulerian summer (May to October) flow from the mean winter (November to April) flow (Figure 7). Over most of the Nordic Seas and the North Atlantic this difference is in the same direction as the mean flow (Figure 5), indicating a winter intensification of the circulation. The increase is largest in the North Atlantic Current and the Norwegian Atlantic Current and partly in the jets associated with topographic features. The winter increase of the flow is on order of 5 cm/s, corresponding to about 20% of the mean flow, but in some areas, such as close to the Norwegian continental slope, it is up to 20 cm/s. The surface currents over the Greenland-Scotland Ridge system also increase, but except for the slope current by less than 5 cm/s. The seasonal difference includes a change in Ekman drift due to the stronger wind stress during winter. According to the NCEP/NCAR reanalysis the seasonal difference in wind speed is about 4 m/s in the Nordic Seas area [*Kistler et al.*, 2001] corresponding to a 2 cm/s ageostrophic signal in an east-westerly direction (section 2.1). However, the drifters seem to follow the bathymetry closely during winter when the ageostrophic motion should be highest, which indicates that the seasonal difference (Figure 7) is mostly geostrophic. The ageostrophic velocity felt by the drifter scales with $\sqrt{N|\tau|/f\rho}$, where N is the Brunt-Väisälä-frequency, τ is the wind stress, ρ is the density of the mixed layer, and f is the Coriolis parameter [*Ralph and Niiler*, 1999]. In the Nordic Seas the upper stratification is mixed away during winter at the same time as the wind stress increases which prevent the ageostrophic movement to grow. This might explain why the drifters are nearly unaffected by the Ekman currents and tend to follow the bathymetry also during winter.

[36] The drifter data set alone is not conclusive to detect, if the winter intensification leads to an enhanced transport across the ridge, or if the water is all recirculated north and south of the ridge system. Current measurements with moored instrumentation, however, indicate that the seasonal variability of the cross-ridge transports, in general, is small [*Hansen and Østerhus*, 2000], although some seasonality of the Atlantic inflow between Scotland and the Faroes has been detected in recent years [*Turrell et al.*, 2001]. The winter intensification of the surface circulation as seen in our drifter analysis and of the transports at selected locations [*Woodgate et al.*, 1999; *Orvik et al.*, 2001] must therefore be primarily linked to spin-up of the local basin gyres. This is clearly seen in the area off the Lofoten Islands near 68°N where some of the boundary current is recirculating as a part of the gyre in the Lofoten Basin (Figure 7a). Also, the

Greenland and the Norwegian basin gyres have spun-up, whereas the situation over the Icelandic plateau is not clear due to the lack of data in the west.

[37] The spin-up of the gyres is supported by the difference in geostrophic velocity calculated from the sea surface height data (Figure 7b) and is also clearly visible in the amplitude and phase distributions of the seasonal signal of sea surface height (Figure 8). The cyclonic gyres in the Norwegian Basin, the Lofoten, and the Greenland basin are spun-up and maximum northward flow is seen along the Scottish and Norwegian shelf break during winter. In addition, the sea surface height shows a clear phase difference across the shelf break between the 200 and 1000 m isobaths, and albeit smaller, across the Greenland-Scotland Ridge (Figure 8). The intensification of the gyres and the area off the Norwegian coast are disconnected and the intensification of the western branch of the Norwegian Atlantic Current is significantly smaller.

[38] A likely reason for the seasonal variability of the circulation is the changing strength of the wind stress forcing over the Nordic Seas (Figure 9). Differences between winter and summer are large, about a factor of four, and during June there is hardly any forcing at all. This oceanic response is not just confined to the frictional surface Ekman layer. The response pattern, like that of the mean circulation, shows an alignment with the local topography, whereas the wind field has a much larger spatial scale, dominated by the Icelandic low. Also, the response seen in the altimeter data is purely geostrophic.

[39] At these high latitudes the seasonal forcing is too rapid to allow a basinwide baroclinic adjustment of the circulation to occur, as it takes first mode planetary waves about 3 years to cross the Nordic Seas. The seasonal response is therefore largely barotropic and consequently strongly controlled by the topography, as observed. In a basin gyre with radius 200 km and 3000 m depth a change in velocity of 5 cm/s corresponds to a transport spin-up of about 30 Sv, not unreasonable when looking at the direct observations [*Woodgate et al.*, 1999] or simple estimates of Sverdrup circulation [*Jónsson*, 1991]. The observed winter intensification of the near-surface circulation internal to the Nordic Seas can thus to a large extent be explained by the increase of the wind-forcing during winter. This does not contradict the low seasonality of the exchanges across the Greenland-Scotland Ridge.

[40] The distribution of the drifter data over 10 years also allows studying interannual variability by comparing the mean circulation during the two periods 1991–1995 and 1996–1999 (Figure 10). These two periods are primarily chosen because of the bi-modal data distribution (Figure 2), but they are also characterized by different wind forcing (Figure 10). In order to prevent these multiyear averages from being biased by the seasonal variability, we show only areas with more than 50 data points during both summer and winter.

[41] South of the Greenland-Scotland Ridge the flow in the Atlantic Current appears to have shifted southward, by a degree or two, during the second half of the decade. As a consequence the zonal flow south of the Faroe Islands has increased, but seems to recirculate southward. This agrees with the finding of *Bersch* [2002] and *Esselborn and Eden* [2001], who saw a change in shape and strength of the

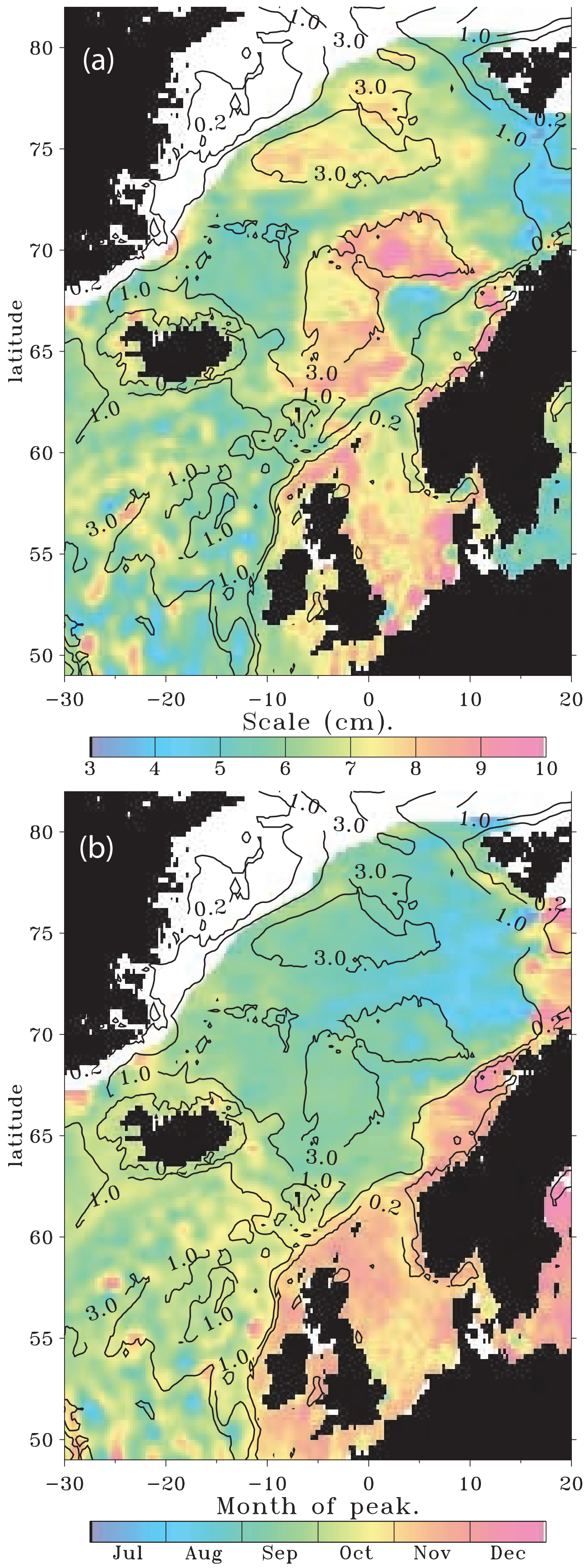

Figure 8. Distribution of (a) amplitude and (b) phase of the seasonal cycle of sea surface height estimated from ERS and TOPEX/Poseidon altimetry from 1992 to 2001.

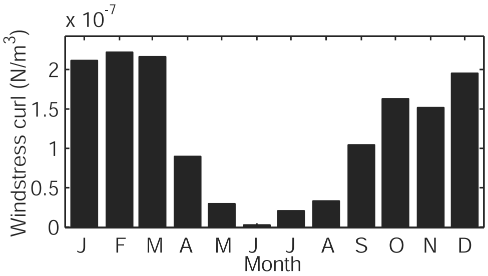

Figure 9. Monthly mean rotation of the wind stress over the Nordic Seas (65°–80°N, 20°W–20°E) derived from the NCEP/NCAR reanalysis data set during the period 1990–2000.

subpolar gyre with the NAO. Our drifter data also indicate that the recirculation in the Island Basin close to the Reykjanes Ridge is larger during the first (NAO-high) period (1991–1995) compared to the second (NAO-low) period (1996–1999). Little or no changes are visible on the ridge, but further north the weakening of the boundary current continues. The Norwegian and the West Spitsbergen currents were 5–10 cm/s stronger during the first period, a signal comparable to the strength of the seasonal variability. In regions of weak mean currents (Figure 5) interannual variability is generally small and scattered in direction. For the eastern boundary currents the weakening toward the second half of the decade can be related to the wind forcing. The wind stress curl over the Nordic Seas during the second half of the 1990s was weaker than during the first half, with a strong minimum during 1995–1996 (Figure 10). Our drifter data are, however, too sparse to allow a separation of these 2 years alone.

[42] We also calculated the difference in sea surface height between the two periods October 1992–December 1993 and April 1995–December 1999 (not shown). In regions of more than about 2 km water depth, sea level rose west and northwest of Norway by 1–5 cm, whereas sea level dropped by 1–7 cm over shallower regions off Norway. This corresponds to a weakening of the NwAtC and West Spitzbergen Current in agreement with the drifter data.

5. Mesoscale Variability

[43] The Norwegian Sea is the birthplace of mesoscale eddies in oceanography. It was here in the Norwegian Atlantic Current where *Helland-Hansen and Nansen* [1909] first observed what they then called "puzzling waves." Mesoscale eddies contribute substantially to the stirring of water masses and thus aid to their mixing. This is in particular so in the Nordic Seas, where the local radius of deformation is small, thus supporting a powerful energy cascade. Here we will discuss the distribution of eddy kinetic energy (Figure 11a) and address the question whether these eddies are formed locally within the gyres, or if they are advected from the energetic boundary current regimes into the interior.

[44] Previous circulation studies in the northern North Atlantic using drifters have typically discussed the distribution of eddy kinetic energy [*Fratantoni*, 2001; *Brügge*, 1995; *Poulain et al.*, 1996a; *Richardson*, 1983]. Here we will invoke additional measures of the mesoscale variability to also discuss eddy-fluxes. Using the temporally filtered velocities the distribution of eddy fluxes $\langle v'u' \rangle$, the off-diagonal of the covariance matrix of $v' = v - \langle v \rangle$, $u' = u - \langle u \rangle$ [*Emery and Thomson*, 2001], is given in Figure 11c. High

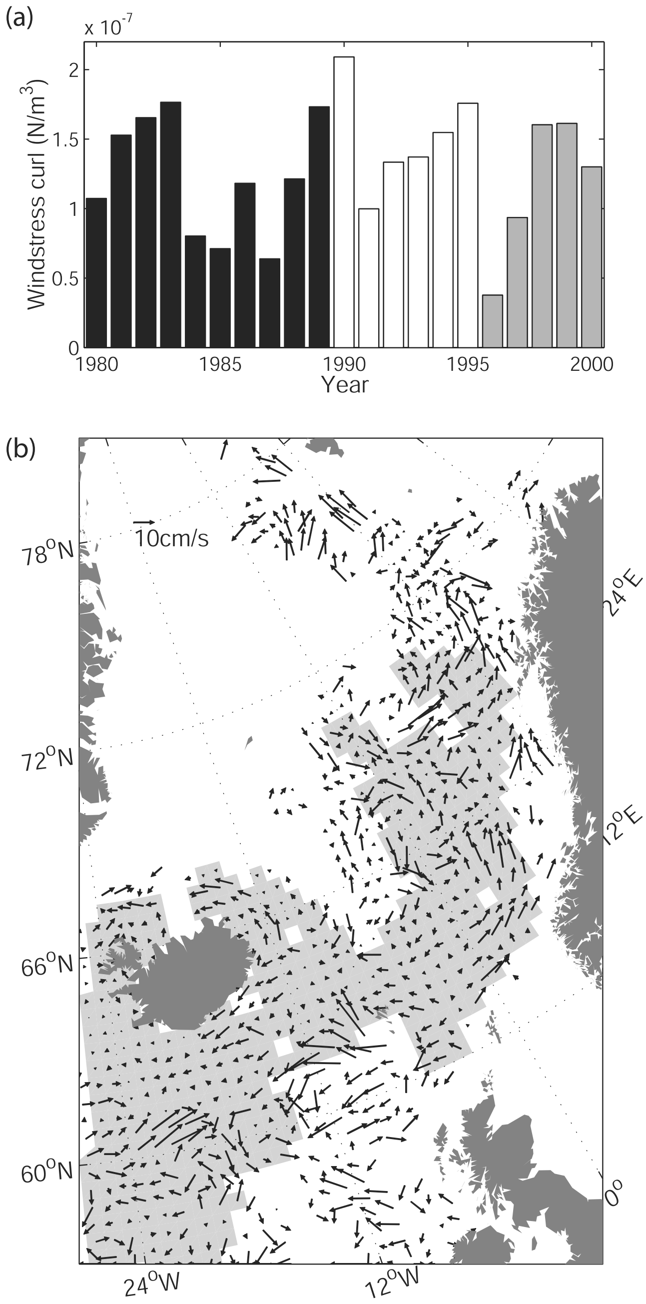

Figure 10. (a) Annual mean rotation of the wind stress over the Nordic Seas (65°–80°N, 20°W–20°E) derived from the NCEP/NCAR reanalysis data set during the period 1980–2000. (b) Interannual variation of the quasi-Eulerian near-surface currents, calculated as the difference between the first (1991–1995) and second part of the decade (1996–1999). Only those regions are shown where at least 50 data points during the respective summer and winter seasons are available during both time intervals. The shading indicates areas where the difference is statistically significant to the 5% level based on the vectorial *t*-test described by *Garraffo et al.* [2001a].

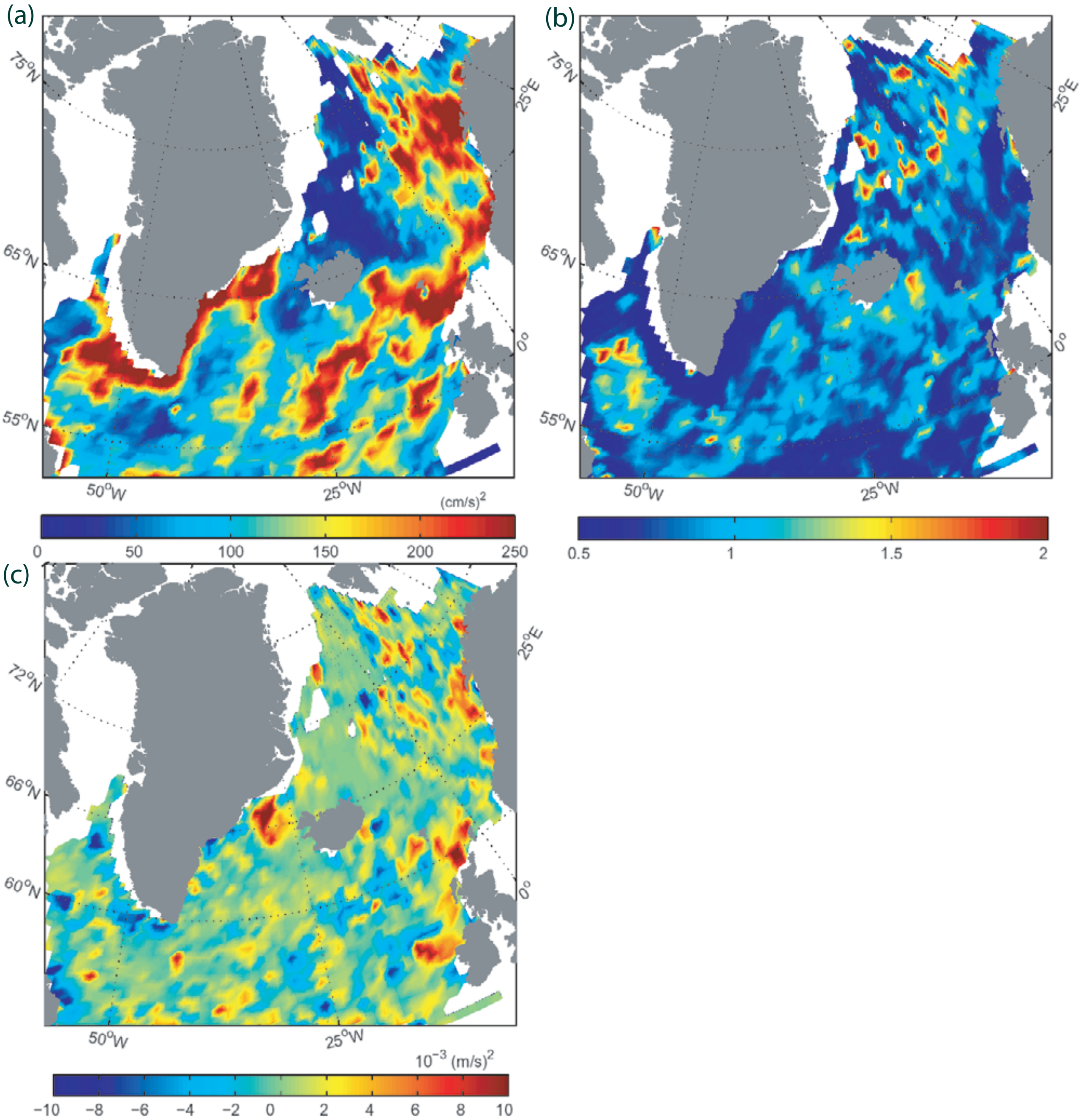

Figure 11. (a) Distribution of the fluctuation or eddy kinetic energy $1/2(\langle u'^2\rangle + \langle v'^2\rangle)$ calculated from the high-pass filtered drifter data. (b) Distribution of the ratio of fluctuation to mean flow as square root of eddy over mean kinetic energies. (c) Distribution of eddy fluxes $\langle v'u'\rangle$.

values are seen in the boundary currents off Norway and Greenland, and the North Atlantic Current off Ireland and Scotland. Basically, this distribution is similar to that of the eddy energy $1/2(\langle u'^2\rangle + \langle v'^2\rangle)$ although high values of $\langle v'u'\rangle$ seem to be more concentrated at the inshore side of the strong boundary currents. The outward gradient in eddy flux means that a net eddy transport occurs from the boundary current regime into the interior. Particularly high values exist off the Lofoten Islands and in Denmark Strait, which is known from other investigations to be a place of very high eddy fluxes. On the other hand, the mesoscale variability seems to follow the energy distribution of the mean flow (not shown). Therefore we look at the ratio of the energy associated with fluctuating motion to the energy associated with the mean flow (Figure 11b). In order to keep the scaling linear, we show the square root of this ratio. As its distribution is equal to that of the energies, we will use this term below.

[45] One can note immediately that the centers of the gyre systems have large eddy to mean energy ratios. This can at least have two reasons: (1) Eddies are locally formed, e.g., through baroclinc instabilities of the frontal regions and the intergyre jets. Convection in the local gyres can also lead to eddy formation, during the breakup of convectively mixed

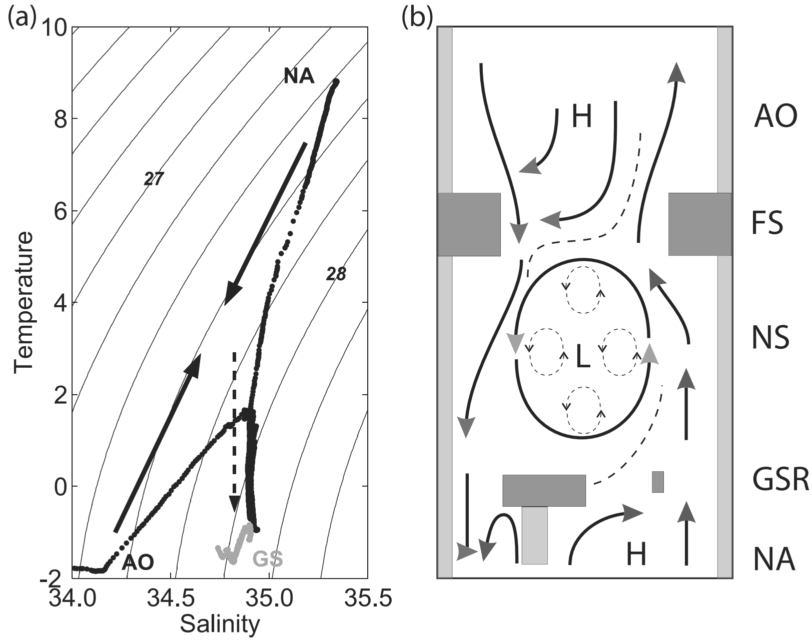

Figure 12. (a) Temperature-salinity diagram of the major water masses in our study area. The hydrographic data were from RV *Oden* in the Arctic Ocean and RV *Valdivia* in the central Greenland Sea and the Faroe Shetland Channel. Abbreviations: NA, North Atlantic; GS, Greenland Sea; AO, Arctic Ocean. (b) Schematic of the large-scale near-surface circulation and location of major fronts (dotted). Abbreviations: FS, Fram Strait; NS, Nordic Seas; GSR, Greenland-Scotland-Ridge; H, high pressure; L, low pressure.

patches [*Marshall and Schott*, 1999; *Steffen and D'Asaro*, 2002]. (2) Mesoscale eddies are advected into the area, and the high eddy to mean energy ratios are due to the low background flow in the area. This would then be an area where the advection of eddies makes a strong impact on the mixing of matermasses. By comparing the ratio of fluctuation to mean flow (Figure 11b) with the distribution of eddy fluxes (Figure 11c) we can get insight into whether eddies are locally formed or if they drift into the area. The regions downgradient of the eddy fluxes will be areas with high eddy to mean energy ratios.

[46] Such an example is the Labrador Sea were the high gradient in the eddy fluxes from the East and West Greenland currents imply a high net advection of eddies into the central Labrador Sea [*Lilly and Rhines*, 2002; *Prater*, 2002]. This then accounts for the high energy ratio seen in the centre of the Labrador Sea (Figure 11b). The high ratios above the Iceland-Faroe Ridge, in contrast, are caused by local eddy formation rather than advection, because the local maxima in the eddy-fluxes coincide with the high ratios seen here. The available potential energy associated with the Polar Front is a powerful source for these mesoscale eddies [*Poulain et al.*, 1996a]. The maximum eddy fluxes just south of Denmark Strait and the high energy ratio also point toward local eddy formation. These can be linked to deep overflow variability [*Käse and Oschliess*, 2000] and have been detected both in situ and with satellite altimetry [*Høyer and Quadfasel*, 2001].

6. Discussion

[47] The near-surface circulation of the Nordic Seas has a relatively simple pattern; it is basically cyclonic and consists of jets and recirculation cells, which are tightly linked to the bottom topography. The large-scale cyclonic wind forcing has a strong seasonal, but also interannual variability, the latter being related to the North Atlantic and Arctic Oscillations [*Dickson et al.*, 2000]. This variable forcing leads to a modulation in the strength of the topographically steered gyres and their interconnecting jets. Currents are stronger during winter and during phases of high NAO Index. The qualitative pattern of the circulation, however, remains the same.

[48] This result is in contrast to recent circulation studies based on hydrographic data from the southern Norwegian Sea, along the Svinøy section at around 63°N [*Blindheim et al.*, 2000]. They report an eastward retreat of the high-salinity Atlantic water regime during the last few decades and relate this to a shift in position or even disappearance of the western branch of the Norwegian Atlantic Current during high NAO conditions [*Blindheim et al.*, 2001]. We cannot confirm that the western branch itself fades away during high NAO Index conditions, as the drifter data do show such a branch, even though the 1990s are characterized by the highest NAO Index conditions of the century.

[49] Since the stratification in our area of the Nordic Seas is weak, the mean circulation closely follows the bottom topography. In fact O. A. Nøst (personal communication, 2002) and P. E. Isachsen (personal communication, 2002) find a circulation pattern very similar to Figure 3 by using a simple theoretical model assuming that f/H contours are closed. However, looking at the distribution of water masses in the Nordic Seas [*Björk et al.*, 2001] it becomes clear that the mean flow cannot account for the overall structure alone. In order to explain the water mass distribution, stirring and mixing processes must be taken into account.

The distribution of the mesoscale variability indicates that eddies are formed at fronts and shed away into the gyre centers (Figure 11b). Here the eddy kinetic energy is relatively large compared to the mean energy. The origin of the eddies is most likely baroclinic instability [*Mysak and Schott*, 1977; *Killworth*, 1980; *Schott and Brock*, 1980].

[50] The variable wind forcing does not seem to cause strong changes in the exchanges between the North Atlantic and the Nordic Seas, but instead mainly affects the circulation internal to the Nordic Seas. Here the narrow boundary currents and the intergyre jets are subject to instability, causing mesoscale current fluctuations. This system of interconnected gyres and the mesoscale eddies causes an effective stirring of polar and Atlantic water masses, which is the prerequisite for strong mixing.

[51] What implications does this have for the large-scale circulation? Figure 12 shows a schematic of the near-surface circulation in the Arctic Ocean, the Nordic Seas, and the North Atlantic Ocean, and characteristic temperature-salinity diagrams of the three basins. The freshwater input through precipitation and river runoff leads to a high water level in the Arctic Ocean compared to the Nordic Seas. The northern pressure head caused by freshwater supply to the Arctic was estimated to be 14 cm by *Rudels* [1987]. It drives the exchange through Fram Strait, with two narrow boundary currents and a cyclonic recirculation of southern water over the sill [*Gill*, 1982; *Rudels*, 1987; *Hunkins and Whitehead*, 1992]. In the south over the Greenland-Scotland Ridge the situation is reversed. The heat loss from the ocean to the atmosphere causes a lowering of the water level in the Nordic Seas compared to that in the North Atlantic. A cooling of Atlantic Water from 8° to 4°C over the top 400 m reduces the steric height by 20 cm. Again, the associated pressure head drives the exchange through two narrow boundary currents and cyclonic recirculation occurs north of the ridge. The presence of topography, in particular of Iceland and the Reykjanes Ridge, disturbs the picture and causes also a recirculation south of the ridge in the Irminger Basin.

[52] The different water levels in the Arctic Ocean, the Nordic Seas, and the North Atlantic drive the circulation sketched in Figure 12b. But now also strong mixing between the Atlantic and Polar water masses occurs in the Nordic Seas, as indicated in the *T*/*S* diagram. When two water columns mix, the steric height of the resulting water column is always less than the mean of those of the two source columns. This is a direct consequence of the nonlinearity of the equation of state. For the extreme case indicated in Figure 12a, the drop amounts to 8 cm, comparable in magnitude to the effect of freshwater input into the Arctic or the cooling effect of the Atlantic water. This means that the mixing in the Nordic Seas by ways of dropping the mean water level also contributes to the large-scale circulation exchanges and circulation. Since the mixing is related to the mesoscale stirring and this again to the local wind-driven circulation, the varying wind forcing does after all have an effect on the Nordic exchanges. Since these exchanges feed back on the overturning circulation, an influence of the local Nordic winds on the global deep circulation cannot be ruled out. This hypothesis and the timescales above which this mechanisms becomes effective can of course not be tested and derived from the data sets on hand, but requires the application of ocean general circulation models. Such models have to be global in order to cover the global circulation, but on the other hand have to resolve the mesoscale dynamics of the Nordic Seas to catch the relevant forcing processes.

[53] **Acknowledgments.** The authors would like to acknowledge scientists contributing data to the drifter Surface Velocity Programme and thank J. Sellschopp formally at SACLANT Undersea Research Centre and T. Dougherty-Poupore at MEDS for making drifter data available. We wish to thank two anonymous reviewers for their constructive comments which helped to improve the paper. Financial support for this study came from the EU projects ESOP and MAIA, the Danish Research Academy, the UK Natural Environment Research Council, and project "OceanKlima" sponsored by the Nordic Council of Ministers.

References

Bacon, S., G. Reverdin, I. G. Rigor, and H. M. Snaith, A freshwater jet on the east Greenland shelf, *J. Geophys. Res.*, *107*(C7), 3068, doi:10.1029/2001JC000935, 2002.

Bersch, M., North Atlantic Oscillation—induced changes of the upper layer circulation in the northern North Atlantic Ocean, *J. Geophys. Res.*, *107*(C10), 3156, doi:10.1029/2001JC000901, 2002.

Björk, G., B. G. Gustafsson, and A. Stigebrandt, Upper layer circulation in the Nordic seas as inferred from the spatial distribution of heat and freshwater content and potential energy, *Polar Res.*, *20*, 161–168, 2001.

Blindheim, J., V. Borovkov, B. Hansen, S.-A. Malmberg, W. Turrell, and S. Østerhus, Upper layer cooling and freshening in the Norwegian Sea in relation to atmospheric forcing, *Deep Sea Res., Part I*, *47*, 655–680, 2000.

Blindheim, J., R. Toresen, and H. Loeng, Fremtidige klimatiske endringer og betydningen for fiskeressursene, *Havets Miljø 2001*, pp. 73–78, Inst. of Mar. Res., Bergen, Norway, 2001.

Brügge, B., Near-surface mean circulation and kinetic energy in the central North Atlantic from drifter data, *J. Geophys. Res.*, *100*, 20,543–20,554, 1995.

Chelton, D. B., R. A. deSzoeke, M. G. Schlax, K. E. Naggar, and N. Siwertz, Geographical variability of the first baroclinic Rossby radius of deformation, *J. Phys. Oceanogr.*, *28*, 433–460, 1998.

Cuny, J., P. B. Rhines, P. P. Niiler, and S. Bacon, Labrador Sea boundary currents and the fate of the Irminger Sea water, *J. Phys. Oceanogr.*, *32*, 627–647, 2001.

Cushman-Roisin, B., and B. Tang, Geostrophic turbulence and emergence of eddies beyond the radius of deformation, *J. Phys. Oceanogr.*, *20*, 97–113, 1990.

Davis, R., Lagrangian and Eulerian measurements of ocean transport processes, in *Ocean Processes in Climate Dynamics: Global and Mediterranean Examples*, edited by P. Malanotte-Rizzoli and A. R. Robinson, pp. 29–69, Kluwer Acad., Norwell, Mass., 1994.

Davis, R. E., Preliminary results from directly measuring mid-depth circulation in the tropical and South Pacific, *J. Geophys. Res.*, *103*, 24,619–24,639, 1998.

Dickson, R. R., and J. Brown, The production of North Atlantic Deep Water: Sources, rates, and pathways, *J. Geophys. Res.*, *99*, 12,319–12,341, 1994.

Dickson, R. R., T. Osborn, J. Hurrell, J. Meincke, J. Bindheim, B. Adlandsvik, T. Vinje, G. Alekseev, and W. Maslowski, The Arctic response to the North Atlantic Oscillation, *J. Clim.*, *13*, 2671–2696, 2000.

Ducet, N., P.-Y. Le Traon, and G. Reverdin, Global high-resolution mapping of ocean circulation from TOPEX/Poseidon and ERS-1 and -2, *J. Geophys. Res.*, *105*, 19,477–19,498, 2000.

Emery, W., and R. Thomson, *Data Analysis Methods in Physical Oceanography*, 2nd ed., 638 pp., Elsevier Sci., New York, 2001.

Esselborn, S., and C. Eden, Sea surface height changes in the North Atlantic Ocean related to the North Atlantic Oscillation, *Geophys. Res. Lett.*, *28*, 3473–3476, 2001.

Fischer, J., and F. A. Schott, Labrador Sea water tracked by profiling floats-From the boundary current into the open North Atlantic, *J. Phys. Oceanogr.*, *32*, 573–584, 2002.

Fratantoni, D. M., North Atlantic surface circulation during the 1990's observed with satellite-tracked drifters, *J. Geophys. Res.*, *106*, 22,067–22,093, 2001.

Garraffo, Z. D., A. J. Mariano, A. Griffa, C. Veneziani, and E. P. Chassignet, Lagrangian data in a high-resolution numerical simulation of the North Atlantic, I, Comparison with in situ drifter data, *J. Mar. Syst.*, *29*, 157–176, 2001a.

Garraffo, Z. D., A. Griffa, A. J. Mariano, and E. P. Chassignet, Lagrangian data in a high-resolution numerical simulation of the North Atlantic, II,

On the pseudo-Eulerian averaging of Lagrangian data, *J. Mar. Syst.*, *29*, 177–200, 2001b.
Gill, A., *Atmosphere-Ocean Dynamics*, *Int. Geophys. Ser.*, vol. 30, 662 pp., Academic, San Diego, Calif., 1982.
Hansen, B., and J. Meincke, Eddies and meanders in the Iceland-Faroe Ridge area, *Deep Sea Res., Part A*, *26*, 1067–1082, 1979.
Hansen, B., and S. Østerhus, North Atlantic-Norwegian Sea exchanges, *Prog. Oceanogr.*, *45*, 109–208, 2000.
Hansen, D., and P.-M. Poulain, Quality control and interpolations of WOCE-TOGA drifter data, *J. Atmos. Oceanic Technol.*, *13*, 900–909, 1996.
Helland-Hansen, B., and F. Nansen, The Norwegian Sea, its physical oceanography based upon the Norwegian researches 1900–1904, in *Report on Norwegian Fishery and Marine Investigations*, vol. 2, 390 pp. + 25 plates, Kristiania, Bergen, Norway, 1909.
Høyer, J. L., and D. Quadfasel, Detection of cold overflows from altimeter satellites, *Geophys. Res. Lett.*, *28*, 1611–1614, 2001.
Hunkins, K., and J. A. Whitehead, Laboratory simulation of exchange through Fram Strait, *J. Geophys. Res.*, *97*, 11,299–11,321, 1992.
Jakobsen, P. K., Meso-scale eddies in the Nordic Seas-Spatiotemporal variability and their relation to deep-sea convection investigated by use of Lagrangian surface drifters, Master thesis, 130 pp., Roskilde Univ., 2000.
Jónsson, S., Seasonal and interannual variability of wind stress curl over the Nordic Sea, *J. Geophys. Res.*, *96*, 2649–2659, 1991.
Kamenkovich, V., M. Koshlyakov, and A. Monin (Eds.), *Synoptic Eddies in the Ocean*, *Environ. Fluid Mech.*, vol. *5*, translated from Russian by V. M. Volosov, 433 pp., D. Reidel, Norwell, Mass., 1986.
Käse, R. H., and A. Oschliess, Flow through Denmark Strait, *J. Geophys. Res.*, *105*, 28,527–28,546, 2000.
Killworth, P., Barotropic and baroclinic instability in rotating stratified fluids, *Dyn. Atmos. Oceans*, *4*, 143–184, 1980.
Kistler, R., et al., *The NCEP-NCAR 50-Year Reanalysis: Monthly Means* [CD-ROM], vol. 82, pp. 247–268, Am. Meteorol. Soc., Boston, Mass., 2001.
Krauss, W., Currents and mixing in the Irminger Sea and in the Iceland Basin, *J. Geophys. Res.*, *100*, 10,851–10,871, 1995.
Lavender, K. L., R. E. Davis, and W. B. Owens, Mid-depth recirculation observed in the interior Labrador and Irminger Seas by direct velocity measurements, *Nature*, *407*, 66–69, 2000.
Le Traon, P.-Y., F. Nadal, and N. Ducet, An improved mapping method of multisatellite altimeter data, *J. Atmos. Oceanic Technol.*, *15*, 522–534, 1998.
Lilly, J. M., and P. B. Rhines, Coherent eddies in the Labrador Sea observed from a mooring, *J. Phys. Oceanogr.*, *32*, 585–598, 2002.
Lumpkin, R., A.-M. Tréguier, and K. Speer, Lagrangian eddy scales in the northern Atlantic Ocean, *J. Phys. Oceanogr.*, *32*, 2425–2440, 2002.
Marshall, J. F., and F. Schott, Open-ocean convection: Observations, theory, and models, *Rev. Geophys.*, *37*, 1–64, 1999.
McCartney, M. S., and C. Mauritzen, On the origin of the warm inflow to the Nordic Seas, *Prog. Oceanogr.*, *52*, 125–214, 2001.
Mork, K., and J. Blindheim, Variations in the Atlantic inflow to the Nordic Seas, 955–996, *Deep Sea Res., Part I*, *47*, 1035–1057, 2000.
Mysak, L. A., and F. Schott, Evidence of baroclinic instability of the Norwegian Current, *J. Geophys. Res.*, *82*, 287–295, 1977.
Niiler, P. P., and J. D. Paduan, Wind-driven motions in the northeast Pacific as measured by Lagrangian drifters, *J. Phys. Oceanogr.*, *25*, 2819–2830, 1995.
Niiler, P., S. Andrew, B. Kenkong, P.-M. Poulain, and D. Bitterman, Measurements of the water-following capability of Holey-Sock and Tristar drifters, *Deep Sea Res., Part I*, *42*, 951–964, 1996.
Orvik, K. A., and P. Niiler, Major pathways of Atlantic water in the northern North Atlantic and Nordic Seas toward Arctic, *Geophys. Res. Lett.*, *29*(9), 1896, doi:10.1029/2002GL015002, 2002.
Orvik, K. A., Ø. Skagseth, and M. Mork, Atlantic inflow to the Nordic Seas: Current structure and volume fluxes from moored current meters, VM-ADCP and SeaSoar-CTD observations, 1995–1999, *Deep Sea Res., Part I*, *48*, 937–957, 2001.
Otto, L., and H. M. Van Aken, Surface circulation in the northeast Atlantic as observed with drifters, *Deep Sea Res., Part I*, *43*, 467–499, 1996.
Pedlosky, J., *Geophysical Fluid Dynamics*, 2nd ed., 710 pp., Springer-Verlag, New York, 1987.
Petterson, O., Die Wasserzirkulation im Nordatlantischen Ozean, *Petermanns Geogr. Mitt.*, *46*, suppl. III and IV, 1–15, 1900.
Pickart, R. S., Is Labrador Sea water formed in the Irminger Sea?, *WOCE Newsl.*, *39*, 6–8, 2000.
Poulain, P.-M., A. Warn-Varnas, and P. Niiler, Near-surface circulation of the Nordic Seas as measured by Lagrangian drifters, *J. Geophys. Res.*, *101*, 18,237–18,258, 1996a.
Poulain, P.-M., P. Zanasca, and A. Warn-Varnas, Drifter observation in the Nordic Seas (1991–1995): Data report, *Data Report SM-299*, NATO SACLANT Undersea Res. Cent., La Spezia, Italy, 1996b.
Prater, M. D., Eddies in the Labrador Sea as observed by profiling RAFOS floats and remote sensing, *J. Phys. Oceanogr.*, *32*, 411–427, 2002.
Ralph, E. R., and P. P. Niiler, Wind-driven currents in the tropical Pacific, *J. Phys. Oceanogr.*, *29*, 2121–2129, 1999.
Rhein, M., J. Fischer, W. M. Smethie, D. Smythe-Wright, R. F. Weiss, C. Mertens, D.-H. Min, U. Fleichmann, and A. Putzka, Labrador Sea water: Pathways, CFC inventory, and formation rates, *J. Phys. Oceanogr.*, *32*, 648–665, 2002.
Richardson, P. L., Eddy kinetic energy in the North Atlantic from surface drifters, *J. Geophys. Res.*, *88*, 4355–4367, 1983.
Rudels, B., On the mass balance of the Polar Ocean, with special emphasis on the Fram Strait, *Norsk Polarinst. Skr.*, *188*, 1–53, 1987.
Schott, F., and M. Brock, Determination of energy interaction terms and horizontal wavelengths for low-frequency fluctuations in the Norwegian Current, *J. Geophys. Res.*, *85*, 4007–4014, 1980.
Stammer, D., On eddy characteristics, eddy transport, and mean flow properties, *J. Phys. Oceanogr.*, *28*, 727–739, 1998.
Steffen, E. L., and E. A. D'Asaro, Deep convection in the Labrador Sea as observed by Lagrangian Floats, *J. Phys. Oceanogr.*, *32*, 475–492, 2002.
Turrell, B., B. Hansen, and S. Øserhus, Hydrographic variability during the decade of the 1990s in the northeast Atlantic and southern Norwegian Sea, paper presented at ICES Meeting, Int. Counc. for Explor. of the Sea, Edinburgh, Scotland, 2001.
Van Aken, H., D. Quadfasel, and A. Warpakowski, The Arctic front in the Greenland Sea during February 989: Hydrographic and biological observations, *J. Geophys. Res.*, *96*, 4739–4750, 1991.
Woodgate, R., E. Fahrbach, and G. Rohardt, Structure and transport of the East Greenland Current at 75°N from moored current meters, *J. Geophys. Res.*, *104*, 18,059–18,072, 1999.

C. W. Hughes, Proudman Oceanographic Laboratory, Bidston Observatory, Bidston Hill, Prenton CH43 7RA, UK. (cwh@pol.ac.uk)

P. K. Jakobsen, M. H. Ribergaard, and T. Schmith, Danish Meteorological Institute, Lyngbyvej 100, DK-2100 Copenhagen, Denmark. (pkj@dmi.dk; mhri@dmi.dk; ts@dmi.dk)

D. Quadfasel, Niels Bohr Institute for Astronomy, Physics and Geophysics, Department of Geophysics, University of Copenhagen, Juliane Maries Vej 30, 2100 Copenhagen Ø, Denmark. (dq@gfy.ku.dk)